

## Quantitative evaluation of iPP nucleation in the presence of carbon fibres: induction time approach

ANITA GROZDANOV<sup>1#</sup>, GORDANA BOGOEVA-GACEVA<sup>1</sup> and MAURIZIO AVELLA<sup>2</sup>

<sup>1</sup>Faculty of Technology and Metallurgy, Rugjer Boskovic 16, Skopje, Macedonia and <sup>2</sup>Instituto di Ricerca e Tecnologia delle Materie Plastiche-CNR, Via Campi Flegrei 34, Comprensorio Olivetti, Fabricato 70, 80078 Pozzuoli, (Napoli) Italy

(Received 15 March 2002)

**Abstract:** Crystallization and nucleation behavior in model composites based on iPP and differently sized carbon fibres have been analyzed in this work. The investigations were performed in the isothermal regime (120–127 °C) using PLM and DSC. The results were analyzed by applying the Avrami and Muchova-Lednický methods. It was shown that the carbon fibre surface acts as a nucleating agent during the crystallization of the iPP matrix. The highest effect was obtained with the fibres of PP-compatible size (C-T) related to unsized carbon fibres (C-U). The induction time,  $t_i$ , and half-time of crystallization decreased with increasing carbon fibre content. The energy effect on the thickness of the critical nucleus decreased in the presence of C-fibres, a fact confirmed by a decrease in the nucleation parameter  $Q$  and the difference energy parameter  $\Delta\sigma$  ( $Q$  decreased from  $-4.96$  for iPP to  $-21.32$  for C/iPP model composites, and  $\Delta\sigma$  decreased from  $6.14 \times 10^{-7}$  J/cm<sup>2</sup> for iPP to  $1.63 \times 10^{-7}$  J/cm<sup>2</sup> for model composites). The results of the model composites and their comparison with published data confirmed that the Muchova-Lednický method could be successfully applied for the quantitative evaluation of the nucleation parameters not only in the temperature range previously suggested (130 – 138 °C), but also at lower crystallization temperatures ( $T_c = 121–127$  °C).

**Keywords:** polypropylene, carbon fibres, crystallization, nucleacion, kinetics.

### INTRODUCTION

Thermoplastic composites, TPC, reinforced with continuous carbon fibres show remarkable improvement of their engineering properties (impact resistance, tensile and flexural strength), and they have found wide application in industry, architecture, etc.<sup>1–3</sup> Among others, the mechanical properties of TPC are influenced by changes in the polymer microstructure, defined by the spherulites size and shapes and the lamellae thickness of spherulites nucleated in the polymer matrix.<sup>4</sup> The nucleation processes and crystalline morphology of the thermoplastic matrix are dependent on the processing conditions, as well as on the type of reinforcing fibre used (carbon, Kevlar, glass).<sup>2–6</sup> Hence, it is of particular interest to perform

# E-mail: ansteg2000@yahoo.com; E-mail: gordana@ereb1.mf.ukim.edu.mk

proper quantitative evaluations of the nucleation process in composites. Carbon fibres (C) are known to induce transcrystallization of some semicrystalline polymer matrices.<sup>5,6</sup> High-modulus carbon fibres (HMCF) induce transcrystallization of PP and PEEK, while high-strength (HTCF), and intermediate-modulus (IMCF) carbon fibres do not.<sup>7,8</sup> The occurrence of transcrystallization is dependent on the topography of the fibre surface and the surface energy, dimensions and orientation of the graphite layers and planes, as well as on the temperature gradient of the interface.<sup>8</sup> Carbon fibres with a fibrillized surface are dominant with regards to transcrystallization. There is an upper critical temperature limit for every fibre, above which the nuclei density is too low to induce transcrystallization. At the same time, and spherulite growth depends on  $T_c$ .<sup>6,8</sup> The importance of chemical interactions in the interface of carbon fibre composites has also been analyzed.<sup>9</sup>

This work is part of a study of model and bulk composites, based on polypropylene, iPP, with carbon or glass fibres. The results of iPP analysis and composites with glass fibres concerning the morphology of the spherulites, as well as the crystallization and melting behavior have already been published.<sup>10-12</sup> It was found that the  $\sigma_e$  values for the iPP matrix, determined by different methods, can differ over a wide range ( $\sigma_e$  (determined by PLM) =  $0.64 \times 10^{-5}$  J/cm<sup>2</sup>,  $\sigma_e$  (determined by DSC) =  $1.80 \times 10^{-5}$  J/cm<sup>2</sup>). The values for the energy parameters obtained from the Avrami equation and DSC data were higher than those obtained from polarizing light microscopy (PML-growth rate measurements). This is attributed to the fact that the analysis of the growth rate is a direct method, whereas the Avrami analysis is more complex and includes different phenomena which influence the results.

In this paper, the results of crystallization and nucleation analysis of iPP composites with differently sized carbon fibres are reported. In order to perform a quantitative analysis of the nucleation processes in C/PP model composites, the obtained experimental data were interpreted by application of the induction time approach.<sup>13-15</sup> The experimental data obtained by two different techniques, polarizing light microscopy and differential scanning calorimetry, were compared.

#### THEORETICAL BACKGROUND

Generally, most crystallization theories are limited to idealized conditions where the temperature and pressure are constant. However, in real processes, the external conditions change continuously, dependent on instantaneous factors. In order to compare traditional studies and theories with the new alternative formulations, an overview of the current state-of-the-art of polymer crystallization is included in this paper.

The classical concept of polymer crystallization involves two independent phenomena: nucleation and growth of the crystalline forms. The crystallization kinetics has been defined by several methods and models, depending on the regime (isothermal or non-isothermal),<sup>16-18</sup> but the most frequently used expression is the Avrami equation (Eq. 1)

$$X = 1 - \exp[-k(T)^n] \quad (1)$$

where:  $X$  is the extent of crystallization,  $k(T)$  is a rate constant,  $n$  is the Avrami exponent. Simultaneously, Johnson and Mehl worked independently on the kinetics of phase trans-

formation, assuming a constant nucleation rate and ignoring the fact that the volume of the untransformed material constantly decreases.<sup>19,20</sup>

For the dynamic regime, the methods of Ozawa (Eq. (2)), Ziabicki (Eq. (3)) and Harnisch and Muschik are usually applied (Eq. (4)).<sup>21-24</sup>

$$X(T) = 1 - \exp[-K_0(T)/C^m] \quad (2)$$

$$C_a = \int_{T_g}^{T_m} K(T) dT = (\pi/\ln 2) K_{\max} D/2 \quad (3)$$

$$n = 1 + [\ln \chi_1/(1-\chi_1) - \ln \chi_2/(1-\chi_2)]/\ln(\beta_2/\beta_1) \quad (4)$$

where: for Eq. (2):  $X(T)$  is the amount of transformation,  $K_0(T)$  is the cooling function of the process,  $C$  is a constant cooling rate and  $m$ ; is the Ozawa exponent, for Eq. (3):  $C_a$  is a parameter known as the kinetic crystallizability,  $K_{\max}$  is the value of  $k$  corresponding to the maximum of the crystallization exotherm,  $D$  is the halfwidth of the crystallization exotherm,  $T_m$  and  $T_g$  are the melting and glass transition temperature, respectively; for Eq. (4):  $n$  is the Avrami exponent,  $\chi_i(t)$  are the derivatives of  $\chi$  which represent  $dH/dT$  values of the exothermic curve,  $\beta_i$  are the heating or cooling rates.

The Ozawa method predicts the kinetics of crystallization during cooling or heating, instead of step crystallization. It was only valid in systems which have a linear dependance of  $\log[-\ln[1-X(T)]]$  against  $\log C$ .<sup>21</sup> Ziabicki extended the Avrami equation in order to predict non-isothermal transformation kinetics of polymers using isothermal transformation data. It was assumed that the slopes of plots of the rate coefficient *versus* temperature are represented by a Gaussian function, which allows the calculation of the parameter  $C_a$ , known as the kinetic crystallizability.<sup>22</sup> Harnisch and Muschik assumed that the enthalpy of transformation is independent of temperature. Some of the possible limitations of the Harnisch-Muschik method are: the Avrami equation must be independent of temperature in the range of the analysis; the heat of fusion of the polymer needs to be known in order to correct the value of  $\chi$ , since polymers are not 100 % crystalline.<sup>23</sup>

Chew and his coworkers developed an integral method of predicting the fraction transformed during non-isothermal crystallization for any arbitrary cooling rate.<sup>24</sup> The advantage of this method is that it uses independently determined nucleation and growth rates. Only one factor was to be integrated: temperature; and the initial and final temperatures of integration must be the same for both the nucleation and spherulite growth rates. If the chosen final temperature is not low enough, the integral method simply cannot describe all the processes of crystallization, especially when the cooling rate is fast.

These models have been tested on almost all semicrystalline polymers. The scientific literature posses a great data base which illuminates the limitations and discrepancies of the models.<sup>25-28</sup> Tobin developed a modification of the Avrami equation, including the growth site impingement of spherulites (Eq. (5)).<sup>26</sup>

$$v_c(t)/(1-v_c(t)) = kt^n \quad (5)$$

where:  $v_c$  is the relative crystallinity,  $k$  is the rate constant and  $n$  is the Avrami exponent. The disadvantages of this model are that secondary crystallization is neglected, and the cooling rate should remain constant during the phase transformation. Cruz-Pinto and his coworkers worked on a modification of the Tobin model in order to account for secondary crystallization.<sup>26</sup> Their model was only valid for isothermal crystallization and it does not differentiate between heterogeneous and homogeneous nucleation. Choe and Lee worked on a modification (Eq. (6)) related to non-isothermal crystallization. This modification accounts for homogeneous and heterogeneous nucleation by their linear combination:<sup>27</sup>

$$v_c(t)/(1-v_c(t)) = [4\pi Nv^3_{\text{het}}t^3]/3 + [I^*v^3_{\text{hom}}t^4]/3 \quad (6)$$

where:  $v_c$  is the relative crystallinity,  $N$  is the number of nucleation sites for heterogeneous nucleation,  $v$  is the radial growth rate of the crystals,  $I^*$  is the nucleation rate. Cebe and Deporter worked on the nucleation models.<sup>29,30</sup> They concluded that heterogeneous nucleation was dominant at lower cooling rates, until the homogeneous nucleation dominates at higher cooling rates, in other words:  $X_{\text{cc},\text{het}} > X_{\text{cc},\text{hom}}$ . In order to include these phenomena precisely and to define a correct value of  $X_{\text{cc}}$ , they defined a new constant  $\zeta$  represented by Eq. (7):

$$\zeta = X_{\text{cc},\text{hom}}/X_{\text{cc},\text{het}} \quad (7)$$

where:  $X_{\text{cc},\text{hom}}$  is the absolute crystallinity at equilibrium under homogeneous nucleation and  $X_{\text{cc},\text{het}}$  under heterogeneous nucleation. This constant represents the dependance of the nucleation mode on the cooling rate.

Recently, a model related to the nucleation mode based on the induction time of crystallization was proposed by Muchova-Lednický.<sup>13–15</sup> According to this concept, the induction time for heterogeneous nucleation,  $t_i$  (Eq. (8)), is the sum of the time necessary for the formation of the first layer on the substrat surface ( $t_h$ ) (Eq. (9)) and the time period for the formation of further layers until the growth of the critical nucleus is completed ( $t_s$ ) (Eq. (10)); the total number of layers corresponds to the critical dimensions  $b_h^*$  of the heterogeneous crystallization nucleus (Eq. (11)).

$$t_i = t_h + t_s \quad (8)$$

$$t_h = A_1 \exp[16\sigma_{b1} \sigma_{ab} \Delta\sigma (T_m^0)^2] / [kT(\Delta H_m \Delta T)^2] \exp(\Delta G_\eta/kT) \quad (9)$$

$$t_s = A_2 [2\Delta\sigma T_o / \Delta H_m \Delta T b_o - 1] \exp[4\sigma_{b1} \sigma_{ab} b_o T_m^0] / [kT \Delta H_m \Delta T] \exp(\Delta G_\eta/kT) \quad (10)$$

$$b_h^* = -2\Delta\sigma / \Delta G_v \quad (11)$$

where:  $A_1, A_2$  are proportionality constants,  $\sigma_{b1}$  and  $\sigma_{ab}$  are the Gibbs specific surface energies of the growing nucleus,  $\Delta\sigma$  is the difference energy parameter,  $T_m^0$  is equilibrium melting temperature,  $\Delta H_m$  is the enthalpy of crystal melting.  $\Delta T$  is undercooling,  $b_o$  is the

thickness of one layer of folding chains,  $\Delta G_\eta$  is the activation energy of diffusion. The equilibrium melting temperature,  $T_m^0$ , was determined by the Hoffman-Weeks method.<sup>3</sup> By using this method, besides  $T_m^0$ , the constant  $\gamma$  is calculated ( $\gamma$  represents the ratio between the final and the initial critical thickness of the crystalline lamellae). As the ratio of the obtained lamellae thickness and the critical thickness of the nuclei, the parameter  $\gamma^*$  is also obtained.

For higher temperatures of crystallization, when the number of folding segments layers is much higher than unity, the time of formation of the first layer ( $t_n$ ) is neglected in relation to the time in which remaining layers are formed, so that the Eq. (8) can be transformed into Eq. (12), or in logarithmic form into Eq. (13).

$$t_s = A_2 [2\Delta\sigma T_m^0 / \Delta H_m \Delta T b_o] \exp[4\sigma_{b1} \sigma_{ab} b_o T_m^0 / [kT \Delta H_m \Delta T] \exp(\Delta G_\eta / kT)] \quad (12)$$

$$\ln(t_i \Delta T) = \ln [C \Delta\sigma T_m^0 / \Delta H_m b_o] + [4\sigma_{b1} \sigma_{ab} b_o T_m^0 / [k \Delta H_m]] [1/T \Delta T] \quad (13)$$

where the influence of a transport term is included in the constant  $C$ . According to Eq. (13), the dependance of  $\ln(t_i \Delta T) - f(1/T \Delta T)$  is a straight line with slope  $K$  (Eq. (14)) and intercept  $Q$  (Eq. (15)):

$$K = 4\sigma_{b1} \sigma_{ab} b_o T_m^0 / k \Delta H_m \quad (14)$$

$$Q = \ln [C \Delta\sigma T_m^0 / \Delta H_m b_o] \quad (15)$$

The values of  $K$  and  $Q$  are determined from experimental measurements of the induction time-dependance on the crystallization temperature. The intercepts,  $Q$ -data give information about the difference energy parameters,  $\Delta\sigma$ . Moreover, by determination of  $K$  and  $Q$  data, it becomes possible to estimate which type of nucleation will dominate, epitaxial or non-epitaxial. For complete analysis of the nucleation density, the following parameters:  $Ke^Q$  and  $e^Q$  have to be included.<sup>14</sup> These nucleation terms result from the equation for the nucleation barrier (Eq. (16)). They were taken into account when the nucleation densities for epitaxial and non-epitaxial nucleation were compared:

$$E = 4Ke^Q / T(\Delta T)^2 C + \ln(C/2A_2) \quad (16)$$

According to Muchova-Lednický, more intensive nucleation is initiated by those nucleation sites which have simultaneously low values of  $Ke^Q$  and  $e^Q$  and high values of parameter  $K$ .<sup>14</sup>

#### EXPERIMENTAL

Melt crystallization and nucleation of iPP in carbon fibre/iPP model composites were analysed by the DSC and PLM techniques. Model composites were prepared using different contents of sized and unsized carbon fibres (5–50 % w/w):(C-Tenax (CU untreated, unsized fibres), and C-Hercules AS4 BASF (CT with thermoplastic compatible size) (see Table I) of the same diameter (7  $\mu\text{m}$ ), and isotactic polypropylene (DAPLEN MT55, Austria, MFI=12–14  $\text{g/m}^2$ ) was used as the matrix.

TABLE I. Basic characteristics of the carbon fibres used in the model composites with iPP

| Fibre | $d/\mu\text{m}$ | $F/(\text{GPa})$ | $E/(\text{GP})$ | $S/(\text{m}^2/\text{g})$ | $a/(\text{mol}/\text{kg})$ | $\rho/(\text{g}/\text{cm}^3)$ |
|-------|-----------------|------------------|-----------------|---------------------------|----------------------------|-------------------------------|
| CU    | 7.6             | 3.5              | 230             | 0.22                      | 0.124                      | 1.75                          |
| CT    | 7.5             | 4.0              | 241             | 0.14                      | 0.158                      | 1.80                          |

Crystallization in the isothermal regime was analysed using a Perkin-Elmer DSC-7. The samples were heated up to 205 °C, held on this temperature for 5 min (to erase the effects of the thermal history) and then cooled to a given crystallization temperature,  $T_c$ , at a cooling rate of 80 °C/min.

Polarizing light microscopy was performed using a Leitz Biomed microscope equipped with a hot-stage and photcamera Nikon-800. Extremely thin samples (*ca.* 0.02 mm) were prepared for analysis by melting the iPP films between two microscope slides (18×18 mm) and then the C fibres were placed in the films. The samples were heated up to 200 °C and then cooled to a given crystallization temperature at a cooling rate of 5 °C/min. Detailed descriptions of the DSC and PLM – measurements are given in Ref. 4. The results were analysed by applying the Muchova-Lednický method.<sup>13-15</sup>

For the quantitative presentation of the slope  $K$  and the intercept  $Q$  from the extrapolation on the dependence  $\ln(t_f\Delta T)$  vs.  $(1/T\Delta T)$ , a computer regression analysis program (STATISTICA v.4.3) was used.

## RESULTS AND DISCUSSION

A comparison of the properties of PP-based composites with differently sized carbon fibres showed an improvement of the mechanical properties (up to 30 %) of the composites reinforced with properly sized fibres.<sup>31</sup> Along with other reasons, the obtained differences resulted from the polymer microstructure formed at proper cooling regimes. Namely, a higher transverse flexural strength was found for CT/PP composites ( $F_{CT/PP} = 6.5 \text{ MPa} > F_{CU/PP} = 4.4 \text{ MPa}$ ) which exhibit siever spherulites network and a higher total grain boundary area per unit volume  $S_v$  ( $S_{vPP} = 22$ ,  $S_{vCU/PP} = 28$ ,  $S_{vCT/PP} = 36$ ).<sup>31</sup> This was the motivation for the further analysis of the crystallization and nucleation processes in the model composites presented in this work.

### Overall crystallization kinetics

From the DSC isothermal crystallization data (Fig. 1) of the model composites and pure PP, the Avrami exponents,  $n$ , and the constant rate of crystallization,  $k$ , were obtained. The results are presented in Table II.

For the studied region (120–127 °C), the exponent  $n$  is approximately 2 (1.81–1.99) for pure PP; similar values were obtained by DiLorenzo:<sup>32</sup>  $T_c = 122\text{--}129 \text{ °C}$ ,  $n = 2\text{--}3$  and Avella and his coworkers:<sup>33</sup>  $T_c = 125\text{--}129 \text{ °C}$ ,  $n = 1.8\text{--}1.9$ . For the C/PP model composites,  $n$  decreased and the obtained values were in the range from 1.0 to 2.7. According to the literature, this result indicates heterogeneous nucleation and two-dimensional growth.<sup>34</sup> The Avrami exponent decreases with increasing fibre content, obviously due to the increased number of crystallization centres.<sup>35,36</sup> Compared with literature data, the obtained values are somewhat lower, and probably should be taken with some reserve, although the same tendency was found by other authors. Feng and his team found that the addition of an appropriate nucleator reduced the Avrami exponent due to changes in the crystallite morphology.<sup>37</sup> Lopez and Arroyo found that unmodified and modified PET fibres decreased the Avrami exponent  $n$  in PET/PP based composites (2.3–1.4).<sup>38</sup>

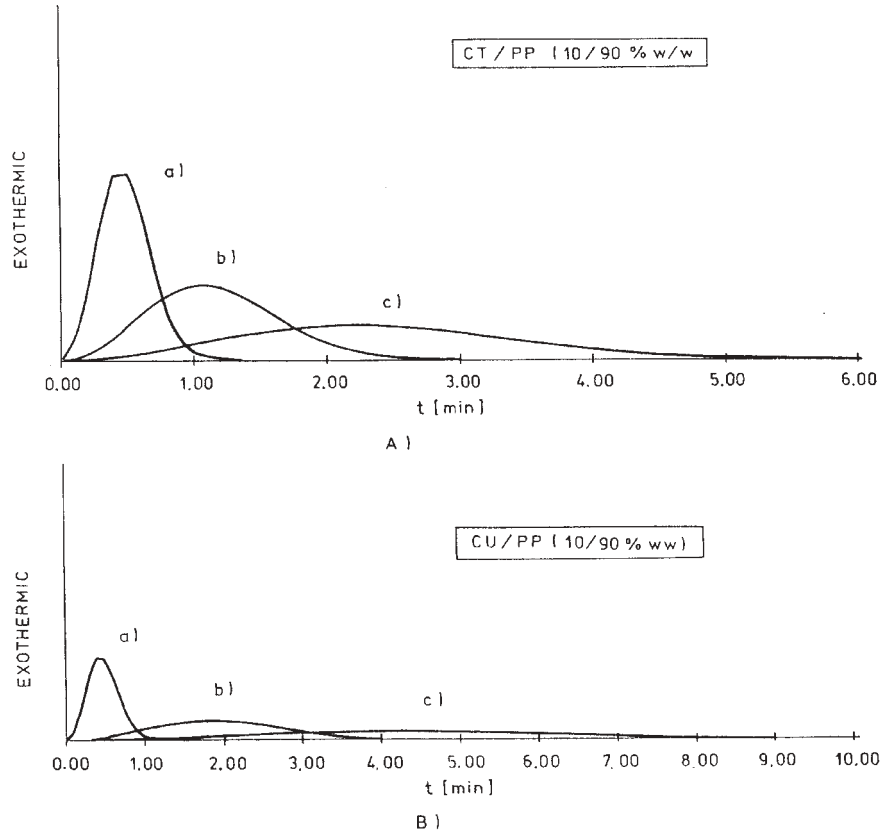


Fig. 1. DSC thermograms of isothermal crystallization for composites at different  $T_c$  (a) 124 °C; (b) 127 °C; (c) 130 °C. A) CT/PP (10/90 % w/w), B) CU/PP (10/90 % w/w).

TABLE II. Avrami exponents,  $n$  and rate constant values,  $k$

| $T$<br>°C | iPP |                      | CU/iPP / % mas |                      |       |                      |       |                      |       |                      |
|-----------|-----|----------------------|----------------|----------------------|-------|----------------------|-------|----------------------|-------|----------------------|
|           |     |                      | 5/95           |                      | 10/90 |                      | 20/80 |                      | 50/50 |                      |
|           | $n$ | $k$                  | $n$            | $k$                  | $n$   | $k$                  | $n$   | $k$                  | $n$   | $k$                  |
| 121       | 1.9 | $2.2 \times 10^{-5}$ | 1.0            | $4.8 \times 10^{-2}$ | 1.0   | $5.4 \times 10^{-2}$ | 1.0   | $4.7 \times 10^{-2}$ | 0.7   | $2.3 \times 10^{-1}$ |
| 124       | 1.8 | $1.3 \times 10^{-5}$ | 1.5            | $6.4 \times 10^{-4}$ | 1.7   | $2.9 \times 10^{-4}$ | 2.7   | $1.0 \times 10^{-5}$ | 1.2   | $1.0 \times 10^{-2}$ |
| 127       | 1.8 | $3.2 \times 10^{-6}$ | 2.0            | $1.2 \times 10^{-5}$ | 2.1   | $6.9 \times 10^{-6}$ | 1.1   | $2.9 \times 10^{-3}$ | 0.9   | $2.5 \times 10^{-2}$ |
| CT/iPP    |     |                      |                |                      |       |                      |       |                      |       |                      |
| $T$<br>°C |     |                      | 5/95           |                      | 10/90 |                      | 20/80 |                      | 50/50 |                      |
|           | $n$ | $k$                  | $n$            | $k$                  | $n$   | $k$                  | $n$   | $k$                  | $n$   | $k$                  |
| 121       |     |                      | 1.2            | $2.7 \times 10^{-2}$ | 1.0   | $5.4 \times 10^{-2}$ | 1.0   | $5.5 \times 10^{-2}$ | 1.3   | $1.1 \times 10^{-2}$ |
| 124       |     |                      | 1.6            | $1.1 \times 10^{-3}$ | 1.3   | $4.7 \times 10^{-3}$ | 1.4   | $4.2 \times 10^{-3}$ | 1.4   | $3.4 \times 10^{-3}$ |

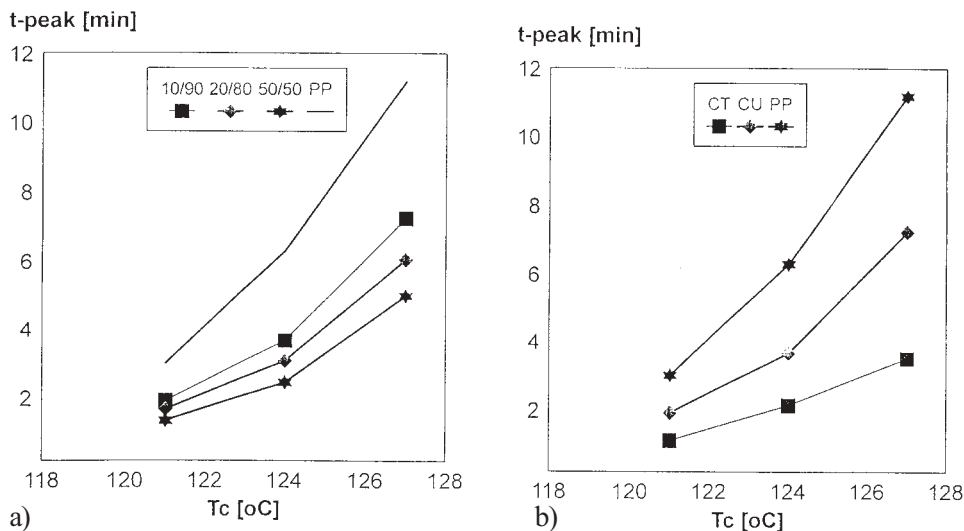


Fig. 2. Dependence of  $t_{peak}$  for the composites on  $T_c$ : a) for different fibre/matrix weight ratios in the CU/PP system; b) for composites with various sized carbon fibres.

127                      2.2     $9.8 \times 10^{-6}$     2.3     $7.4 \times 10^{-6}$     2.3     $9.6 \times 10^{-6}$     2.0     $4.9 \times 10^{-5}$

The changes of  $t_{peak}$  are shown in Fig. 2a for different carbon fibre contents and in Fig. 2b for various carbon fibres. The experimental measurements showed that  $t_{peak}$  decreases with increasing carbon fibre content ( $\Delta t_{peak} \approx 2$  min); especially low values for  $t_{peak}$  were obtained for CT ( $\Delta t_{peak} \approx 4$  min in comparison with CU/iPP model composites) for  $T_c = 124; 127^\circ\text{C}$ .

The changes of the half-time of crystallization,  $t_{0.5}$  are presented in Fig. 3. It can be

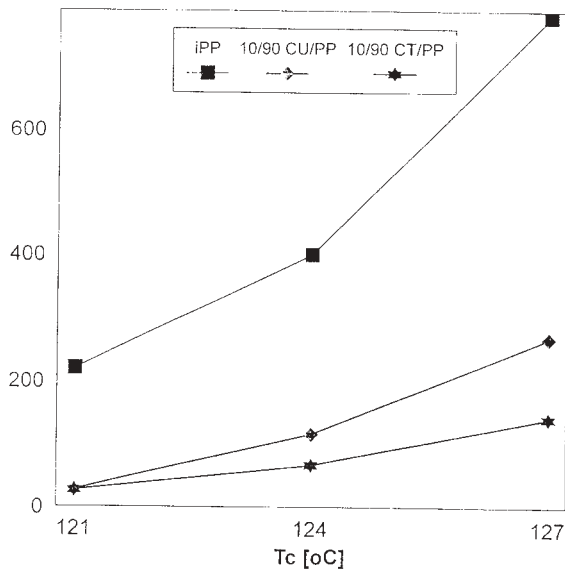


Fig. 3. Dependence of  $t_{0.5}$  on  $T_c$  in the presence of differently sized C fibres.

seen that  $t_{0.5}$  has a lower value in the presence of CT. The obtained results for  $t_{\text{peak}}$  and  $t_{0.5}$  indicate that the crystallization of the matrix in model composites was initiated and proceeds at higher rate, especially in the presence of sized fibres, CT.

#### *Nucleation mode in C/PP model composites*

The differences noticed during crystallization in the model composites are probably due to differences in the nucleation density and nucleation processes. Therefore, an attempt

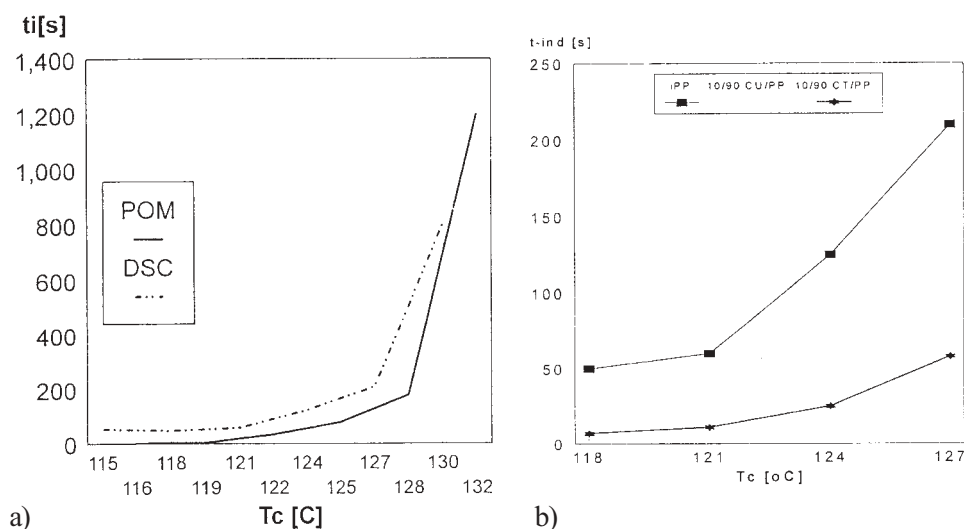


Fig. 4. Dependence of the induction time of PP and the composites on  $T_c$ .

was made to analyse the nucleation mode in more detail in these systems.

The changes of the induction time,  $t_i$ , are presented in Fig. 4. The lower values of  $t_i$  in the presence of carbon fibres indicates an increased nucleation ability of the matrix for nucleation and shorter periods of formation of critical nuclei. The induction time values for the model composites with untreated unsized C fibres, CU were higher than for CT fibres. This confirms that the nucleation processes in the CT/iPP model composites commenced earlier. Our previous investigations showed the effect of the surface chemistry of the fibre: CT fibres with a compatible size exhibit a higher adsorption capacity in comparison to unsized,  $a_{CT} = 0.158$  mol/kg,  $a_{CU} = 0.124$  mol/kg (Table I) which indicates a high number of active centres and their possible influence on the interface chemistry; FTIR and XPS spectra showed the presence of reactive functional groups (CONH-,  $-\text{NO}_2$ -) in surface sites of the fibres.<sup>36</sup> The results for  $t_i$  obtained by PLM and DSC measurements have analogous trends, although insignificantly higher values were obtained by DSC analysis, due to the fact that direct observation of the changes occurring during the nucleation processes is extremely difficult, even impossible. According to theory, the character of this type of curves for the induction time dependance on the crystallization temperature suggests the existence of two types of nucleation sites, with different surface energies, but having an identical influence on the structure of the nuclei.<sup>14,15</sup> Besides theoretical analysis, interpretation of  $t_i$ -curves is connected with many problems, because some of the physical pa-

rameters have still not been quantitatively determined.

*Application of the Muchova-Lednicky induction time approach*

Using the Muchova-Lednicky method, an attempt was made to characterize the dependence of  $t_i$  on the formation of first layer of nuclei, represented by the function  $\ln(t_i) - f(1/T\Delta T)^2$ , and the dependence of  $t_i$  on the formation of the next layer of the crystal nuclei

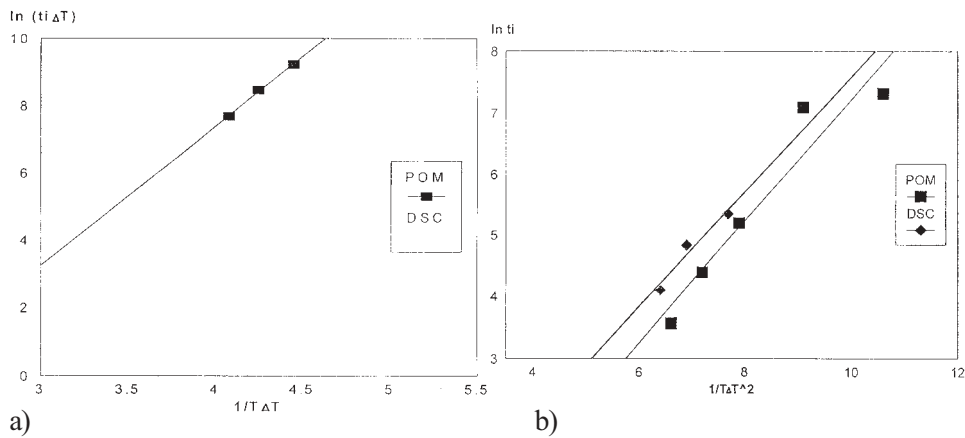


Fig. 5. a) Dependence of  $\ln(t_i\Delta T)$  on  $1/T\Delta T$  for the pure PP matrix. b) Dependence of  $\ln t_i$  on  $1/T\Delta T^2$  for the pure PP matrix.

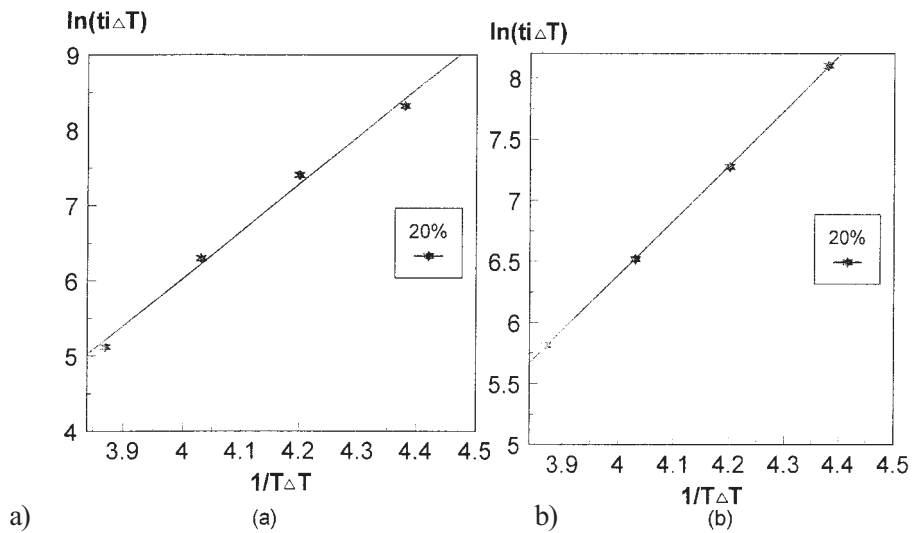


Fig. 6. Dependence of  $\ln(t_i\Delta T)$  on  $1/T\Delta T$  for the composites with differently sized C fibres: a) CU/PP composites; b) CT/PP composites.

with the time, represented by the function  $\ln(t_i\Delta T) - f(1/T\Delta T)$ .

The corresponding results obtained by both techniques (PLM and DSC) are presented

in Fig. 5a and Fig. 5b (for pure iPP), and in Fig. 6a and Fig. 6b (for model composites). These relations, which were introduced by Ishida, should be linear over the studied temperature range.<sup>39</sup> For the pure iPP matrix, linearity was confirmed in the temperature range from 121 to 128 °C ( $1/T\Delta T = (40 - 45)\times 10^{-6} \text{ K}^{-2}$ ), which is in agreement with literature data for iPP.<sup>14</sup> Linearity was also confirmed for the model composites in the range (121–127 °C) and for fibre contents of 5, 10, 20 %. This fact suggests that this method could also be applied for crystallization temperature ranges below 130 °C. According to the induction time theory, during crystallization below  $T_c < 135$  °C, the time of formation of the first layer (which changes more with  $T_c$  than the time of the formation of the remaining layers of the crystal nuclei), is most important. This was deduced from the decrease in the number of layers in the critical nuclei with decreasing  $T_c$ .<sup>13,14</sup> The slope  $K$  and the intercept  $Q$  of the extrapolation of the function  $\ln(t_i\Delta T) - f(1/T\Delta T)$  were determined. These parameters were used for the quantitative evaluation of some of the nucleation characteristics. The obtained results based on DSC and PLM – measurements are reported in Table III.

TABLE III. Energetic parameters determined according to the Muchova-Lednický method<sup>14</sup>

| Composite/(technique) | $K \times 10^5$ | $Q$    | Corr. coeff. | $e^Q$                 | $Ke^Q$               |
|-----------------------|-----------------|--------|--------------|-----------------------|----------------------|
| iPP/(PLM)             | 4.14            | -9.18  | 0.998        | $1.0 \times 10^{-4}$  | $4.3 \times 10^1$    |
| CU/iPP (PLM)          | 4.56            | -12.67 | 0.996        | $3.1 \times 10^{-6}$  | $1.4 \times 10^0$    |
| CT/iPP (DSC)          | 4.69            | -12.83 | 0.994        | $2.6 \times 10^{-6}$  | $1.2 \times 10^0$    |
| iPP/(DSC)             | 3.28            | -4.96  | 0.992        | $7.2 \times 10^{-3}$  | $2.4 \times 10^3$    |
| 5 % CU/iPP (DSC)      | 5.90            | -17.01 | 0.990        | $4.0 \times 10^{-8}$  | $2.4 \times 10^{-2}$ |
| 10 % CU/iPP (DSC)     | 6.89            | -21.32 | 0.980        | $5.5 \times 10^{-10}$ | $3.7 \times 10^{-4}$ |
| 20 % CU/iPP (DSC)     | 5.77            | -16.94 | 0.990        | $4.3 \times 10^{-8}$  | $2.4 \times 10^{-2}$ |
| 5 % CT/iPP (DSC)      | 4.05            | -9.64  | 0.974        | $6.5 \times 10^{-5}$  | $2.6 \times 10^1$    |
| 10 % CT/iPP (DSC)     | 4.45            | -11.43 | 0.999        | $1.1 \times 10^{-5}$  | $4.9 \times 10^0$    |
| 20 % CT/iPP (DSC)     | 4.52            | -11.73 | 0.999        | $8.0 \times 10^{-6}$  | $3.6 \times 10^0$    |

The registered higher values for  $K$  in the model composites, as well as the lower values of  $e^Q$  and  $Ke^Q$  were obviously due to favoured nucleation. The results are comparable with the literature data.<sup>14</sup> The slope  $K$  determined from the DSC data was higher than those based on the PLM data  $(5.9-6.8)\times 10^5$  for CU fibres and  $(4.0-4.5)\times 10^5$  for CT fibers.

#### *Effect of equilibrium melting temperature*

The evaluation of the  $K$  and  $Q$  parameters including the undercooling term  $\Delta T = T_m^0 - T_c$  confirmed the effect of the equilibrium melting temperature,  $T_m^0$ , on the nucleation parameters. The values of  $T_m^0$  for PP published in the literature vary greatly. Muchova and Lednický checked the importance of  $T_m^0$  – variation in the evaluation of the  $\ln(t_i\Delta T) - f(1/T\Delta T)$  dependence. They found that, depending on the  $T_m^0$  – used, this function would not vary significantly, if  $T_m^0$  did not differ markedly. So, they assumed that this error is not

significant.<sup>15</sup> Also, they pointed out that when the structure of the nuclei is modified by the surface structure of the filler, changes in the measured  $T_m^0$  could be expected. The obtained values for  $T_m^0$ ,  $\gamma$  and  $\gamma^*$ , determined from DSC data are presented in Table IV.

TABLE IV. Equilibrium melting temperature,  $T_m^0$  and constants  $\gamma/\gamma^*$  determined from DSC-data for the model composites

| Carbon fibre content/% | CT/iPP     |          |            | CU/iPP     |          |            |
|------------------------|------------|----------|------------|------------|----------|------------|
|                        | $T_m^0$ /K | $\gamma$ | $\gamma^*$ | $T_m^0$ /K | $\gamma$ | $\gamma^*$ |
| 0                      | 457.1      | 2.7      | 2.7        | 457.1      | 2.7      | 2.7        |
| 5                      | 455.3      | 3.1      | 3.2        | 458.2      | 2.8      | 2.9        |
| 10                     | 455.9      | 3.0      | 3.1        | 455.4      | 3.1      | 3.1        |
| 20                     | 459.0      | 2.7      | 2.8        | 456.5      | 2.9      | 3.0        |
| 50                     | 456.1      | 2.9      | 3.0        | 457.6      | 2.8      | 2.8        |

The value of  $T_m^0$  showed a decreasing tendency on addition of both fibres to the PP matrix, although it tends to increase with increasing fibre content. Similar variation were found for PP model composites with PET and PA fibres.<sup>38</sup> Namely, the determined value for  $T_m^0$  of PP decreases on addition of PET and PA fibres, and increases as the degree of the fibre modification increases. Obviously, these values should be taken with some reserve since two-phase composite materials do not present ideal conditions, and comparison of this characteristic among the composite and pure polymer is not adequate.

The parameters  $\gamma$  and  $\gamma^*$  were also changed in the presence of C-fibres. Similar results were presented in literature, where  $\gamma$  increased with glass fibre content.<sup>40</sup> These changes in  $\gamma$  and  $\gamma^*$  data (known as morphological parameters), express the morphological changes of the polymer due to the nucleation activity of the fibres.

#### *Nucleation-morphology relations*

For non-epitaxial nucleation, the  $K$  parameter has the same value and changes in its value are connected with the epitaxial structure of the nuclei.<sup>15</sup> Comparison of our results showed that, independent of the applied technique, the  $K$  parameter exhibits similar values for all model composites. This fact indicates a non-epitaxial mechanism of nucleation. PLM analysis of these composites did not prove the existence of a transcrystalline layer, although it is known that epitaxial nucleation does not always yield transcrystallization. Individual growth of spherulites is sometimes also possible.<sup>15</sup>

The parameter  $Q$  decreased with increasing fibre content. According to the Muchova-Lednický method, the physical meaning of a decreasing tendency of  $Q$  is an increased nucleation efficiency due to the fibres and an increased nucleation density. Namely, although non-epitaxial nucleation was assumed, using the  $Q$  parameter it is possible to determine ability of a surface to initiate nucleic and, at the same time, to obtain the density of the nucleation sites. The increased nucleation activity of the fibre surface was confirmed by an

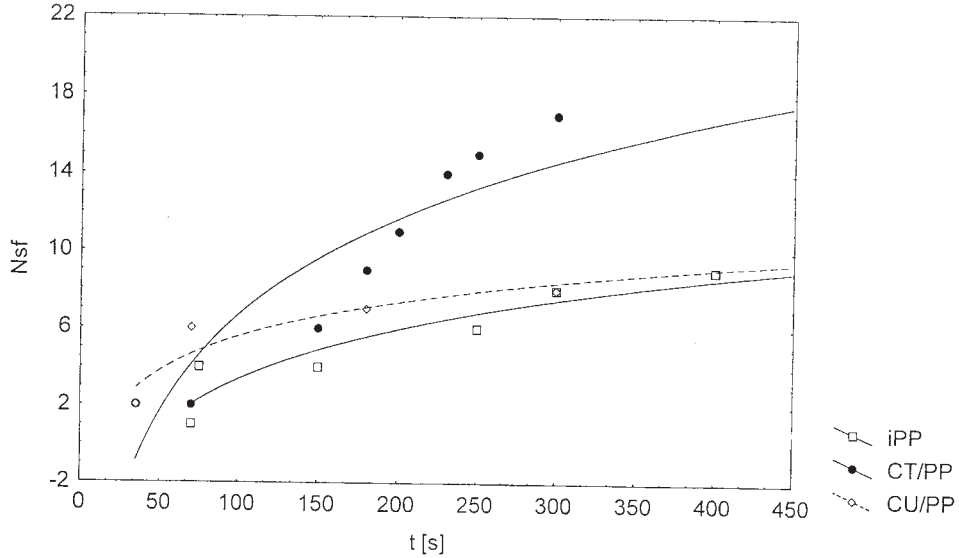
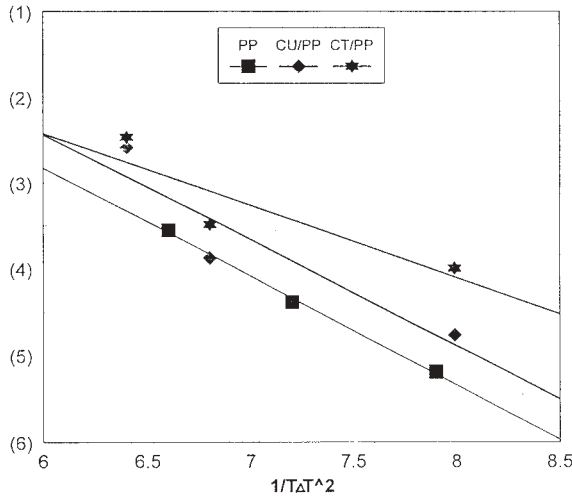


Fig. 7. Number of spherulites versus time during isothermal crystallization at  $T_c = 125\text{ }^\circ\text{C}$ .

increased number of spherulites (Fig. 7).

*Analysis of the interfacial energy parameters*

Using the slope  $K_i$  of the dependance  $\ln(t_i) - f(1/T(\Delta T)^2)$ , Fig. 8, interfacial energy parameters, such as the surface energy parameters  $\sigma\sigma_a\Delta\sigma$  and  $\sigma\sigma_c$ , the crystal fold surface



neous nucleation,  $\Delta\sigma$  is represented by:  $\Delta\sigma = \sigma + \sigma_m - \sigma_c$  where  $\sigma$  is the free surface energy of formation of a lateral crystal,  $\sigma_m$  is the substrate-melt interfacial energy and  $\sigma_c$  is the substrate-crystal interfacial energy. The decreasing value of  $\Delta\sigma$  with increasing fibre content confirmed the nucleation efficiency.<sup>2,14</sup> The CT fibres showed lower values for  $\Delta\sigma$  ( $\Delta\sigma = 1.63 \times 10^{-7} \text{ J/cm}^2$ ) than the unsized CU fibres ( $\Delta\sigma = 2.60 \times 10^{-7} \text{ J/cm}^2$ ). Obviously certain surface treatments might favour the nucleation processes. Compared with the literature data for the  $\Delta\sigma$ -values of other fibres, such as Kevlar ( $\Delta\sigma = 3.35 \times 10^{-7} \text{ J/cm}^2$ ), PTFE ( $\Delta\sigma = 0.75 \times 10^{-7} \text{ J/cm}^2$ ), and PET ( $\Delta\sigma = 5.87 \times 10^{-7} \text{ J/cm}^2$ ), the obtained values confirmed the nucleation efficiency of the fibres used.<sup>2,14,41</sup> However, it should be pointed out that a lot of different methods for the determination of interfacial energy parameters by thermal analysis are used indiscriminately in the literature. The experimentally obtained values for the energy parameters have shown that they strongly depend on the technique and method used for their calculation: kinetic and nucleation parameters determined from DSC data are higher than those obtained by PLM. Ishida tested the induction time hypothesis on a system where  $\Delta\sigma$  can be measured from both the nucleation rates and the induction time. The difference between the value of  $K_i$  determined by the two approaches was 9 %, which was largely due to the uncertainty in the origin of time.<sup>42</sup> The interfacial energy parameters determined by the two methods showed a more significant difference, 15.5 %.<sup>41</sup> According to Calli and Zanoto, the secondary phenomena that can occur during crystallization (thickening, exclusion of low molecular weight fractions, *etc.*) are disregarded in an Avrami

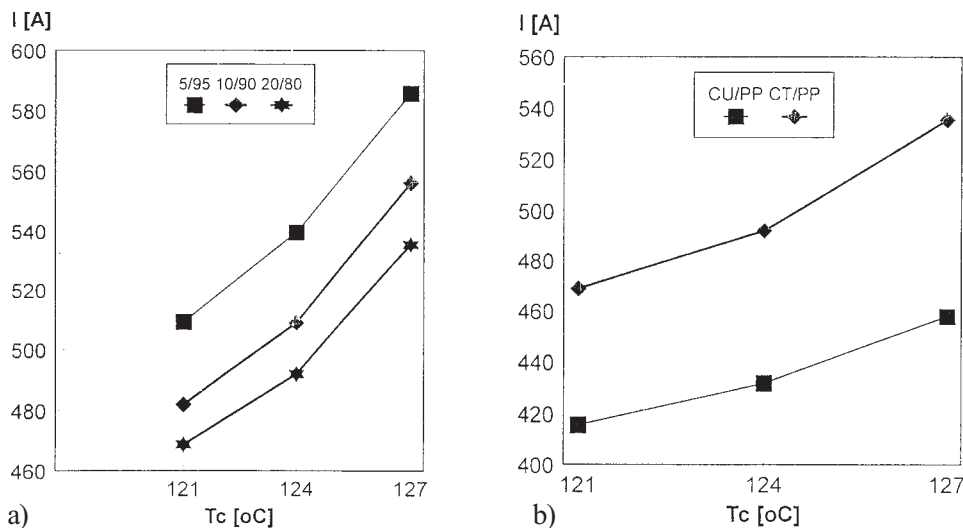


Fig. 9. Lamellae thickness,  $l$  versus  $T_c$ : a) for various C fibre contents (CT/PP composites); b) for differently sized C fibres.

analysis: the straight line of an Avrami plot includes only the primary crystallization.<sup>41</sup>

The changes of the lamellae thickness at different  $T_c$  are presented in Fig. 9. The effect of the fibre/matrix interface is confirmed by the fact that the lamellae thickness is higher in

the presence of CT. The obtained values are in the range of 370 to 550 Å and are comparable with the results of Greso and Phillips.<sup>25</sup> According to their investigations, medium-modulus C fibres (such as CT) promote thicker lamella and do not induce transcrystallization.

#### CONCLUSION

Using the methods of Avrami and Muchova-Lednický, a quantitative evaluation of the basic nucleation energy parameters in C/iPP model composites was performed. Based on the induction time approach (applying PLM and DSC) different values for the nucleation parameters were registered in the presence of variously treated carbon fibres. It was shown that the influence of energy on the critical nucleus thickness was released in the presence of carbon fibres, confirmed by a decrease of the nucleation parameter  $\Theta$  from  $-4.96$  for iPP to  $-21.32$  for C/iPP model composites. CT sized fibres showed lower values for  $\Delta\sigma$  ( $\Delta\sigma = 1.63 \times 10^{-7}$  J/cm<sup>2</sup>) than unsized CU fibres ( $\Delta\sigma = 2.60 \times 10^{-7}$  J/cm<sup>2</sup>), which confirmed that a certain surface treatment of the fibres favours the nucleation processes. The experimentally obtained data for all the energy parameters showed a strong dependence on the technique used for their determination. The results for the C/PP composite systems and their comparison with published data, confirmed that the Muchova-Lednický method can be successfully applied for the quantitative evaluation of nucleation parameters not only in the temperature range suggested by the authors, but also at lower crystallization temperatures ( $T_c = 121\text{--}127$  °C).

#### LIST OF SYMBOLS

- $X$  – Extent of crystallization
- $k(t)$  – Rate constant
- $n$  – Avrami exponent
- $m'$  – Ozawa exponent
- $t$  – Time
- $C$  – Constant Ozawa cooling rate
- $Ca$  – Kinetic crystallizability
- $K_{\max}$  – Value of the Ziabicki rate constant at maximum crystallization rate
- $D$  – Half-width of the crystallization exotherm peak
- $T_c$  – Crystallization temperature
- $T_m$  – Melting temperature
- $T_g$  – Glass transition temperature
- $T_m^0$  – Equilibrium melting temperature
- $\Delta T$  – Undercooling ( $T_m^0 - T$ )
- $\Delta H_m$  – Enthalpy of crystal melting
- $\gamma$  – Constant representing the ratio between the final thickness of crystalline lamellae and initial critical thickness
- $\gamma^*$  – Constant representing the ratio between the obtained lamellae thickness and the critical thickness of the nuclei
- $\chi_i$  – Crystal conversion
- $\Phi_i$  – Heating or cooling rates
- $\nu_c$  – Relative crystallinity

$N$  – number of nucleation sites for heterogeneous nucleation  
 $\nu$  – Radial growth rate of crystals  
 $I^*$  – Nucleation rate  
 $X_{\infty, \text{hom}}$  – Absolute crystallinity at equilibrium under homogeneous nucleation  
 $X_{\infty, \text{het}}$  – Absolute crystallinity at equilibrium under heterogeneous nucleation  
 $\zeta$  – Cebe-Deporter constant of the nucleation mode  
 $t_i$  – Induction time  
 $t_{0.5}$  – Half-time of crystallization  
 $t_h$  – Time necessary for the formation of the first layer on the substrate surface  
 $t_s$  – Time period for the formation of future layers until the growth of the critical nucleus is completed  
 $A_1, A_2, C$  – Constants of proportionality  
 $\sigma_b, \sigma_{ab}$  – Gibbs specific surface energies of the growing nucleus  
 $\Delta\sigma$  – Difference energy parameter  
 $\sigma$  – The free surface energy of formation of a lateral crystal  
 $\sigma_e$  – Crystal fold surface energy  
 $\sigma_m$  – Substrate-melt interfacial energy  
 $\sigma_c$  – Substrate-crystal interfacial energy  
 $\Delta G_\eta$  – Activation energy of diffusion  
 $b_0$  – Thickness of one nucleus layer  
 $Q, K$  – Parameters for the quantitative evaluation of the nucleation of the material  
 $E$  – Nucleation barrier

## ИЗВОД

 КВАНТИТАТИВНА ЕВАЛУАЦИЈА НУКЛЕАЦИЈЕ РР У ПРИСУСТВУ  
 УГЉЕНИЧНИХ ВЛАКАНА: МЕТОДОМ ИНДУКЦИОНОГ ВРЕМЕНА

 АНИТА ГРОЗДАНОВ<sup>1</sup>, ГОРДАНА БОГОЕВА-ГАЦЕВА<sup>1</sup> и MAURICIO AVELLA<sup>2</sup>
<sup>1</sup>Технолошко-металуршки факултет, Рибар Бошкових 16, Скопје, Македонија и <sup>2</sup>Istituto Nazionale per lo Studio e l'Utilizzazione di Polimeri e Compositi, Via Campi Flegrei 34, Komprensorio Olivetti, Fabrikato 70, 80078 Poggioreale, (Napoli), Italy

У овом раду анализиране су кристализација и нуклеација моделних композита на бази РР ојачаног угљеничним, С, влакнима са различитим површинским премазом. Испитивања су изведена у изотермалном режиму (120–127 °C), користећи PLM и DSC. Резултати су анализирани применом Avrami-јеве и Muhova-Lednicki методе. Показано је да се површина С влакана понаша као нуклеатор током кристализације РР матрице. Најбољи ефект је постигнут са С влакнима са компатибилним премазом. Индукционо време,  $t_i$ , и полупериод кристализације,  $t_{0.5}$ , опадају са повећањем садржине угљеничних влакана. Енергетски ефект дебљине критичног нуклеуса опада у присуству С влакана, што је потврђено опадањем нуклеационог параметра  $Q$  и енергетског параметра  $\Delta\sigma$  ( $Q$  опада од – 4.96 за iPP до – 21.32 за С/РР композит;  $\Delta\sigma$  опада од  $6.14 \times 10^{-7}$  J/cm<sup>2</sup> за iPP до  $1.63 \times 10^{-7}$  J/cm<sup>2</sup> за композит). Резултати испитивања С/РР моделних композита у овом раду, као и подаци из литературе, потврђују да метода Muhova-Lednicki може успешно да се користи за квантитативну евалуацију нуклеационих параметера не само у температурном режиму предложеном од аутора (130–138 °C), већ и код нижих температура кристализације ( $T_c = 121 - 127$  °C).

(Примљено 15. маја 2002.)

## REFERENCES

1. E. Mader, U. Bunzel, M. Schemme, *Techtextil Symposium* (1993) P316

2. M. Avella, E. Martuscelli, B. Pascuccu, M. Raimo, *Polym. Eng. Sci.* **32** (1992) 383
3. J. L. Thomason, A. A. Van Rooyen, *J. Mater. Sci.* **27** (1992) 889
4. A. Grozdanov, G. Bogoeva-Gaceva, *14<sup>th</sup> Bratislava Conference on the Tailoring of the Properties of Thermoplastic Composites and Blends*, 1–4 October, Bratislava, P39, (2000) p. 142
5. A. J. Greso, P. J. Phillips, *J. Advan. Mater.* (1994) July 51
6. J. Varga, J. Karger-Kocsis, *Polymer* **36** (1995) 4877
7. R. H. Burton, M. J. Folkes, *Plast. Rub. Process. Appl.* **3** (1983) 129
8. Y. Cai, J. Petermann, H. Wittich, *J. Appl. Polym. Sci.* **65** (1997) 67
9. J. Danault, *ICCI-V*, Geteborg (1994) P15-1
10. A. Janevski, G. Bogoeva-Gaceva, *J. Appl. Polym. Sci.* **69** (1998) 381
11. G. Bogoeva-Gaceva, A. Janevski, A. Grozdanov, *J. Appl. Polym. Sci.* **67** (1998) 395
12. A. Grozdanov, G. Bogoeva-Gaceva, *J. Serb. Chem. Soc.* **63** (1998) 455
13. M. Muchova, F. Lednicky, *J. Macromol. Sci.-P.B.* **34** (1995) 55
14. M. Muchova, F. Lednicky, *Polymer* **37** (1996) 3037
15. M. Muchova, F. Lednicky, *Polymer* **37** (1996) 3031
16. B. Wunderlich, *Macromolecular Physics*, Academic Press, New York, 1976
17. F. L. Binsbergen, *J. Polym. Sci. Polym. Phys. Ed.* **11** (1973) 117
18. Y. Long, R. a. Shanks, Z. H. Stachurski, *Prog. Polym. Sci.* **20** (1995) 651
19. M. Avrami, *J. Chem. Phys.* **8** (1940) 212
20. W. A. Johnson, R. F. Mehl, *Trans.AIME* **135** (1939) 416
21. T. Ozawa, *Polymer* **12** (1971) 150
22. A. Ziabecki, *Colloid Polym. Sci.* **252** (1974) 433
23. K. Harnisch, H. Muschik, *Colloid. Polym. Sci.* **261** (1983) 908
24. S. Chew, Z. H. Stachurski, J. R. Griffiths, L. F. R. Rose, *Polymer 91 Conf. Proc.*, 1991, p. 272
25. R. Philips, J. E. Manson, *J. Polym. Sci. B* **35** (1997) 875
26. M. C. Tobin, *J. Polym. Sci., Polym. Phys. Ed.*, **12** (1974) 399
27. C. R. Choe, K. H. Lee, *Polym. Eng. Sci.* **29** (1989) 801
28. A. M. Chatterjee, F. R. Price, *J. Polym. Sci., Poly. Phys. Ed.* **13** (1975) 2391
29. P. Cebe, L. Lowry, S. Y. Chung, A. Yavrouian, A. Gupta, *J. Appl. Polym. Sci.* **34** (1987) 2273
30. K. Deporter, D. G. Baird, D. G. Wilkes, *J. M. S.-Rev. Macro. Chem. Phys.* **C33** (1993) 1
31. A. Grozdanov, G. Bogoeva-Gaceva, *ICCM-13*, Beijing (2001) 25–29 June
32. L. DiLorenzo, C. Silvestre, *Prog. Polym. Sci.* **24** (1999) 917
33. M. Avella, E. Martuscelli, C. Selliti, E. Caraganani, *J. Mater. Sci.* **22** (1987) 3185
34. L. Mendelkern, *Crystallization of Polymers*, McGraw-Hill, New York, 1964
35. C. Wang, L. M. Hwang, *J. Polym. Sci., B* **34** (1996) 47
36. A. Grozdanov, D. Burevski, G. Bogoeva-Gaceva, *16<sup>th</sup> Congress of the Chemists and Technologists of Macedonia*, 28 – 30 October, 1 (1999) 211
37. Y. Feng, X. Jin, J. N. Hay, *J. Appl. Polym. Sci.* **69** (1998) 2089
38. M. A. Lopez-Manchado, M. Arroyo, *Polymer* **40** (1999) 487
39. H. Ishida, P. Bussi, *Macromolecules* **24** (1991) 3569
40. G. Bogoeva-Gaceva, A. Janevski, E. Mader, *Polymer* **42** (2001) 4409
41. A. Celli, E. Zanotto, *Thermochim. Acta* **269/270** (1995) 191
42. C. Wang, C. R. Liu, *Polymer* **38** (1997) 4715.